Direct Observation of the Layer-By-Layer Growth of Initial Oxide Layers on Si(100) Surface during Thermal Oxidation

V. D. Borman, E. P. Gusev, Yu. Yu. Lebedinskii, and V. I. Troyan
Moscow Engineering Physics Institute, Moscow 115409, U.S.S.R.
(Received 8 February 1991)

We present the results of an x-ray photoelectron spectroscopy investigation in the real-time regime of the kinetics of high-temperature oxidation of the Si(100) surface. The dependence of the net concentration of silicon atoms in all oxidation states (i.e., Si^{1+}, Si^{2+}, Si^{3+}, Si^{4+}) on oxygen exposure is found to exhibit a "step"-like behavior, each "step" corresponding to one oxide layer. The results obtained suggest a mechanism of layer-by-layer growth of initial oxide layers, with oxide-phase formation taking place at the Si-SiO_2 interface.

PACS numbers: 81.60.Cp, 82.65.Jv, 82.80.Pv

It was proposed recently [1,2] that the unique electrophysical characteristics of the Si-SiO_2 interface are likely determined by the formation kinetics of the transition region in thermal oxidation. However, the mechanism of formation of this transition region between silicon crystal and bulk SiO_2 has yet been revealed, despite extensive study [2,3]. The reason for an atomically abrupt Si-SiO_2 interface is not understood either. The composition and structure of the transition region have been investigated previously. In particular, Grunthaner *et al.* [4], and subsequently others [5-11], found in Si $2p$ photoelectron spectra peaks attributed [4,5] to silicon atoms in different oxidation states, i.e., Si^{1+}, Si^{2+}, Si^{3+}, and Si^{4+}. The role of these states in oxide formation is still under discussion. In this Letter we report results which demonstrate for the first time that the growth of initial oxide monolayers proceeds by a layer-by-layer growth mechanism. Initially, there is accumulation of silicon atoms in Si^{1+} and Si^{2+} states at the interface, which is then followed by their transition into Si^{3+} and Si^{4+} at a constant quantity of silicon atoms in all Si^{n+} states. This quantity stands for one oxide layer.

The experiments were carried out on the XSAM-800 spectrometer (the energy resolution is 0.9 eV). The x-ray photoemission spectrometry method was used (Mg $K\alpha$ source). The electron binding energy was measured with 0.1-eV reproducibility. The oxidation kinetics was investigated directly in the analyzer chamber in a real-time regime [12], contrary to the usually used [6,13] point-by-point regime after a certain exposure. Admitting oxygen into the chamber ($p=10^{-6}$ Torr), we registered Si $2p$ and O $1s$ spectra one by one every 3 min. The sample temperature of 1135 K was chosen in accordance with the conventional silicon-oxidation regime [1-3]. The spectrum of Si $2p$ recorded after oxidation, along with the result of its decomposition into components by least-squares fitting after background subtraction, is depicted in Fig. 1. The peaks corresponding to Si^{1+}, Si^{2+}, Si^{3+}, and Si^{4+} states are shifted by 1.0, 1.7, 2.6, and 3.8 eV, respectively, towards higher binding energies relative to the substrate Si $2p$ peak (99 eV). These shifts are consistent with the results of previous studies: 0.6, 1.5, 2.8, and 4.5 eV (Ref. [4]); 1.0, 1.8, 2.7, and 3.5 eV (Ref. [5]); 1.0, 1.7, 2.6, and 3.6 eV (Ref. [6]); 0.95, 1.79, 2.48, and 3.9 eV (Ref. [7]); and 1.0, 1.7, 2.6, and 3.8 eV (Ref. [8]).

Figure 2 illustrates the accumulation of silicon atoms in different Si^{n+} states during oxidation. To visualize the dependences, we summed the concentrations of Si atoms in Si^{1+} and Si^{2+} states (given by the Si12 line), and in Si^{3+} and Si^{4+} states (Si34 line). The sum of the concentrations of all four states (Si_Σ line) is the quantity of Si atoms with broken Si-Si bonds occupied by different numbers of oxygen atoms. The intensity of the Si_Σ line is the area under the whole spectral line excluding the area corresponding to the substrate Si $2p$ peak, i.e., the area

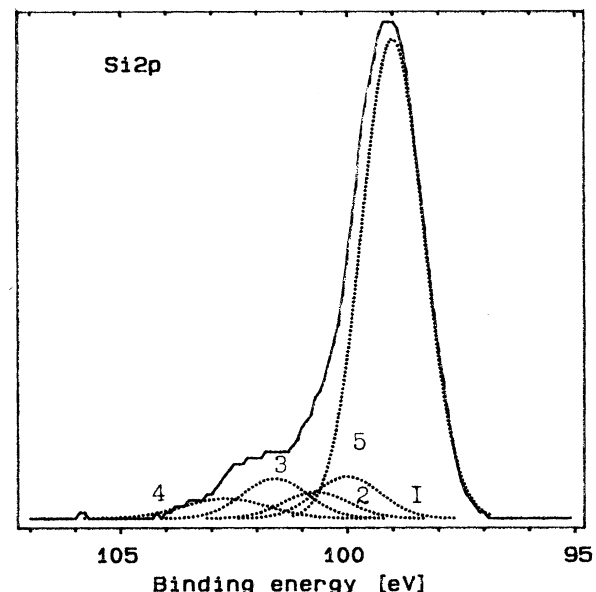

FIG. 1. Si $2p$ photoelectron spectrum recorded after oxidation for 30 min at 1135 K. Curve 1, Si^{1+}; curve 2, Si^{2+}; curve 3, Si^{3+}; and curve 4, Si^{4+}. The substrate Si $2p$ peak (curve 5) is formed by a $2p_{3/2}$,$2p_{1/2}$ doublet with 0.6-eV splitting and an intensity ratio of about 2:1. The form of all lines is Gaussian.

© 1991 The American Physical Society

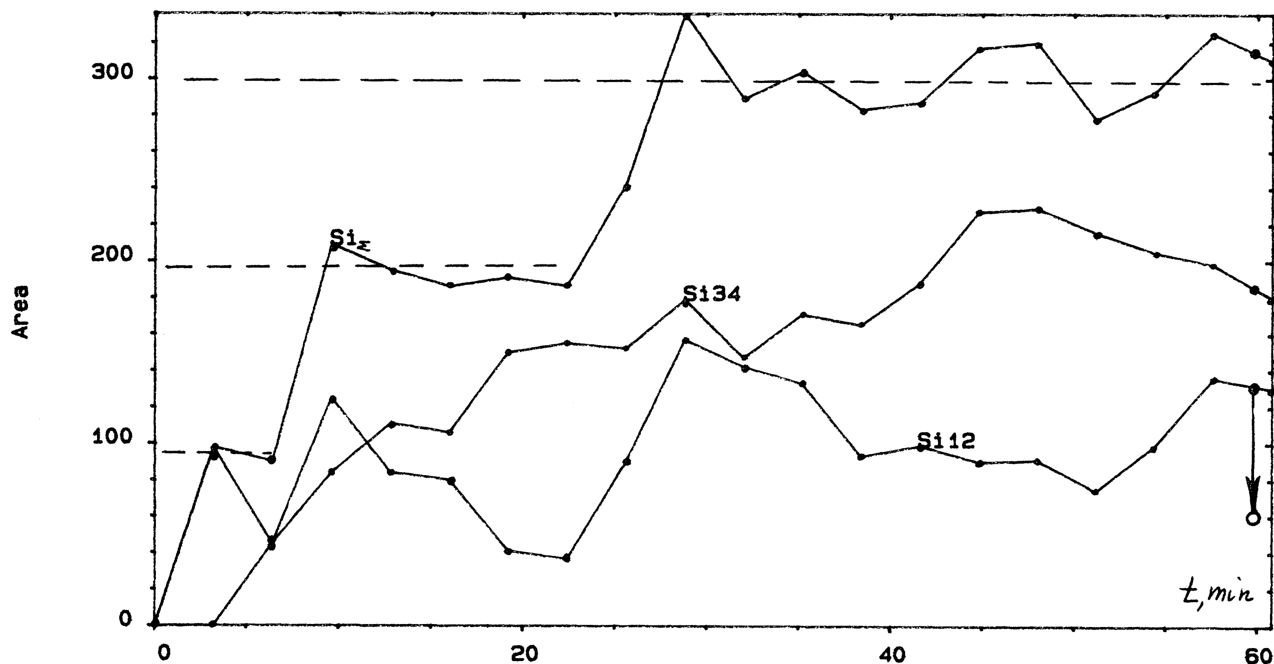

FIG. 2. Kinetics of the accumulation of silicon atoms in different oxidation states during initial oxidation (solid circles). The arrow indicates that the Si^{1+}, Si^{2+} states decrease (open circle) by UHV annealing. The curve Si_Σ represents the concentration of silicon atoms in all four oxidation states, i.e., the sum of Si^{1+}, Si^{2+}, Si^{3+}, and Si^{4+} states.

restricted to the shoulder (see Fig. 1). In this context, it should be emphasized that the Si_Σ intensity does not depend on the Si^{1+}, Si^{2+}, Si^{3+}, and Si^{4+} peak positions. It can be seen from Fig. 2 that the Si_Σ line has three "steps," with Si $2p$ photoelectron integrated intensities equal to 100, 200, and 300 arbitrary units, respectively. To determine the Si-atom concentrations corresponding to these intensities we used the fact that clean silicon yields an intensity of $I_{Si}=2000$ arbitrary units. In the case of a normal photoelectron detection angle being used in the experiment, the value of I_{Si} is determined by the equation $I_{Si}=\int_0^\infty I_0 \exp(-z/\lambda_{Si})dz=I_0\lambda_{Si}$, where z is the distance from the surface, λ_{Si} is the $2p$ photoelectron escape depth in silicon (for the Mg $K\alpha$ source $\lambda_{Si}=13$ Å [14]), and I_0 is the intensity from the surface silicon atoms per length unit. Taking into account the value of the interlayer spacing for Si(100) of 1.36 Å it can be easily calculated that the substrate Si $2p$ signal (I_{Si}) is contributed by approximately ten silicon layers. Thus, one surface atomic layer in silicon yields (when exponential attenuation is negligible) a signal with an intensity of about 200 arbitrary units. Now, it should be noted that the Si-atom concentration in silicon (4.99×10^{22} cm^{-3}) is approximately 2 times greater than in silica (2.3×10^{22} cm^{-3}). That is why one oxide layer corresponds to a Si $2p$ photoelectron signal intensity of about 100 arbitrary units [15]. It is such an intensity that corresponds to the step height in Fig. 2. Therefore we conclude that the steps of the Si_Σ line result from sequential formation of oxide layers on the Si(100) surface, with each of these three steps corresponding to one oxide monolayer. Oxidation at $T=1135$ K for a period of 60 min yields three oxide monolayers (see Fig. 2). This number of layers is in good agreement with the value obtained separately by means of an O $1s$ photoelectron intensity calibration.

Now we consider the redistribution of silicon atoms among different states during the oxidation by comparing Si12, Si34, and Si_Σ lines in Fig. 2. In the initial period ($t<3$ min), Si^{3+}, Si^{4+} states do not appear. Thus the increase of the Si_Σ signal is entirely due to the appearance and accumulation of Si^{1+}, Si^{2+} states. Then, within the time period from 3 to 6 min, the quantity of silicon atoms in all oxidation states (i.e., Si_Σ) remains nearly constant and corresponds to one oxide monolayer. Simultaneously, the Si12 line goes down while the Si34 line goes up. In other words, a transition of silicon atoms from Si^{1+}, Si^{2+} states to Si^{3+}, Si^{4+} states occurs, which completes the oxide monolayer formation. During the Si_Σ concentration increase up to the value of the second step, corresponding to two oxide layers ($6<t<9$ min), Si^{1+}, Si^{2+}-state accumulation again takes place. At the step $t=9$–21 min, these states transform into Si^{3+}, Si^{4+} ones again. A similar result is valid for the third step also (i.e., the accumulation of the Si^{1+}, Si^{2+} states at $t=21$–27 min and their transformation into Si^{3+}, Si^{4+} states at $t=27$–60 min). After 60 min of oxidation (the end of the third step), the quantity of Si^{1+}, Si^{2+} states is still significant in comparison with Si^{3+}, Si^{4+}. However, annealing in

the UHV conditions ($p=10^{-9}$ Torr) at $T=1135$ K for 15 min brings about a twofold decrease in the concentration of silicon atoms in Si^{1+}, Si^{2+} states (see the arrow in Fig. 2). It is noteworthy that this decrease is due to a drastic decrease in the Si^{1+} state, whereas the Si^{2+} changes only within 15%. Moreover, the Si^{2+} concentration increases during annealing.

Thus one may conclude that the oxide monolayer formation is accompanied by the accumulation of the Si^{1+}, Si^{2+} states followed by their transition into Si^{3+}, Si^{4+} at a constant quantity of silicon atoms in all Si^{n+} states (Si_{Σ} line). Such a behavior is characteristic of each oxide layer growth, in particular, of the first oxide monolayer, where the existence of the step at 3–6 min is less convincing because there are only two points depicted in Fig. 2.

The experimental data obtained suggest the following mechanism of initial silicon-oxide-layer formation during thermal oxidation. The growth of each layer can be divided into two stages. The first is connected with oxygen-atom accumulation at the interface. Silica growth is found [1,3–16] to proceed by oxygen (rather than silicon) diffusion [17], with the silicon-oxide formation occurring at the Si-SiO_2 interface. This accumulation is accompanied by Si^{1+}, Si^{2+}-state formation. The results of the experiments [7–11] carried out on oxide films with thicknesses of 10–50 Å do confirm the localization of Si^{1+} and Si^{2+} states in the narrow [from 2 Å (Ref. [11]) to 6–10 Å (Ref. [8])] near-interface region. At the second stage, on achieving a definite interfacial oxygen concentration (or silicon atoms in the Si^{1+} and Si^{2+} states), a first-order phase transition takes place. This result in the appearance of the silicon atoms in Si^{3+} and Si^{4+} states and the decrease of the Si^{1+}, Si^{2+} states. In accordance with Refs. [12,18,19], surface oxide formation is frequently accompanied by structural transformation in the surface layer of the substrate. It takes a certain finite phase-transition time (τ_{PT}) for the new (oxide) phase to form. It follows that the phase transition cannot be finished in a real-time experiment because of the short measurement time (τ_{exp}) as compared to τ_{PT}. As a result, the Si^{1+}, Si^{2+} concentration does not drop to zero (Fig. 2) within the time intervals corresponding to the steps, especially the third step. A quite different situation takes place after UHV annealing. Now the times τ_{PT} and τ_{exp} seem to become comparable, giving rise to the decrease in the Si^{1+}, Si^{2+} states actually observed in the experiment (arrow in Fig. 2). The conversion of Si^{1+}, Si^{2+} to Si^{3+}, Si^{4+} upon annealing was also observed by Hollinger and Himpsel [5]. The formation of the new phase at a first-order phase transition is known [20] to arise from nucleation and island growth. Indeed, oxide microcrystallites of 100-Å size were observed by high-resolution transmission electron microscopy [16] for an oxide film (19 Å thickness) grown in an oxygen environment on Si(100). Finally, it should be noted that the proposed layer-by-layer oxide growth mechanism permits us to understand why thermal oxidation results in an atomically abrupt Si-SiO_2 interface.

In summary, we emphasize that the experimental data elucidate the mechanism of interfacial oxygen transformation into oxide during very-thin-film growth. The transformation is shown to proceed by a first-order phase transition. This interpretation agrees quite favorably with the results obtained recently by Ourmazd and coworkers [21,22]. They observed by high-resolution transmission electron microscopy a thin (5 Å) crystalline oxide phase located between Si(100) crystal and vitreous silica. It was proposed that the most likely candidate for this phase is tridymite [21–23]. On proving the existence of the intermediate crystalline phase, Ourmazd and coworkers logically suggested that silicon oxidation is accompanied by a transition of the diamond-cubic–wurzite-hexagonal type occurring at the interface. This statement is consistent with our model where structural tranformation takes place during initial silicon oxidation. According to the Ourmazd structural model of the SiO_2/Si(100) interface, the Si^{1+} and Si^{2+} states are interfacial dimers and Si-O-Si bridges, respectively (see Fig. 6 in Ref. [22]). The drastic decrease of the Si^{1+} state as well as the increase of the Si^{2+} state during UHV annealing indicates that the phase transition proceeds as follows. The interfacial Si-Si bond (dimer) is broken (the Si^{1+} decrease) and a diffused oxygen atom binds with these two silicon atoms resulting in a Si-O-Si bridge (Si^{2+} state). As for the Si^{3+} state, Chu and Fowler [24] showed within the framework of the Ourmazd model that the Si^{3+} configuration was connected with an oxygen vacancy in the near-interfacial oxide. In accordance with the reactive-layer model [25,26] proposed for the initial ($d<50$ Å) silicon oxidation, a thin oxide grows at the stage of reactive-layer formation by means of oxygen-atom diffusion through the silica network via oxide defects. In terms of this model, the experimental data obtained correspond to the stage of reactive-layer formation. The observation of the Si^{3+} state does confirm the existence of oxide defects (oxygen vacancies), which according to Stoneham, Grovenor, and Cerezo [25] and Mott *et al.* [26] should play an important role in oxygen transport during initial oxidation. However, it is rather difficult to say something about the validity of the reactive-layer model in general because of the small oxide thickness achieved in the experiment (up to 5 Å).

The authors are grateful to Dr. A. V. Emelyanou, Dr. Yu. N. Devyatko, Dr. V. N. Tronin, and Dr. A. P. Popov for their fruitful discussions, and Dr. P. A. Alexandrov for support and discussions.

[1] E. Irene, CRC Crit. Rev. Solid State Mater. Sci. **14**, 175 (1988).

[2] C. L. Claeys, R. F. De Keermaecker, and G. J. Declerck,

in *The Si-SiO₂ System,* edited by P. Balk (Elsevier, Amsterdam, 1988).

[3] A. Atkinson, Rev. Mod. Phys. **57**, 437 (1985).

[4] F. J. Grunthaner, P. J. Grunthaner, R. P. Vasquez, B. F. Lewis, J. Maserjian, and A. Madhukar, Phys. Rev. Lett. **43**, 1683 (1979).

[5] G. Hollinger and F. J. Himpsel, Phys. Rev. B **28**, 3651 (1983); J. Vac. Sci. Technol. A **1**, 640 (1983).

[6] M. Tabe, T. T. Chiang, I. Lindau, and W. E. Spicer, Phys. Rev. B **34**, 2706 (1986).

[7] F. J. Himpsel, F. R. McFeely, A. Taleb-Ibrahimi, J. A. Yarmoff, and G. Hollinger, Phys. Rev. B **38**, 6084 (1988).

[8] P. J. Grunthaner, M. H. Hecht, F. J. Grunthaner, and N. M. Johnson, J. Appl. Phys. **61**, 629 (1987).

[9] T. Hattori and T. Suzuki, Appl. Phys. Lett. **43**, 470 (1983).

[10] A. Ishizaka and S. Iwata, Appl. Phys. Lett. **36**, 71 (1980).

[11] N. Aoto, E. Ikawa, N. Endo, and Y. Kurogi, Surf. Sci. **243**, 121 (1990).

[12] V. D. Borman, E. P. Gusev, Yu. Yu. Lebedinskii, A. P. Popov, and V. I. Troyan, Zh. Eksp. Teor. Fiz. **95**, 1378 (1989) [Sov. Phys. JETP **68**, 795 (1989)].

[13] F. Lutz, J. L. Bischoff, L. Kubler, and D. Bolmont, Phys. Rev. B **40**, 10356 (1989).

[14] M. F. Hochella, Jr., and A. H. Carim, Surf. Sci. **197**, L260 (1988).

[15] The Si $2p$ photoelectron signal attenuation in oxide is negligible during initial oxide-layer growth since the thickness of oxide after oxygen exposure of 60 min (5 Å) is substantially less than the $2p$ photoelectron escape depth in silica ($\lambda_{SiO_2}=21$ Å, Ref. [14]). The oxide thickness was estimated using the current intensities of Si $2p$ signals from the substrate and from silicon atoms in all oxidation states, and the value of λ_{SiO_2}.

[16] F. Rochet, S. Rigo, M. Froment, C. d'Anterroches, C. Maillot, H. Roulet, and G. Dufour, Adv. Phys. **35**, 2356 (1986).

[17] The nature of the diffusing species depends on the oxide film thickness. It is conventionally accepted [Refs. [1-3,16] and A. M. Stoneham, C. R. M. Grovenor, and A. Cerezo, Philos. Mag. B **55**, 201 (1987); N. F. Mott, S. Rigo, F. Rochet, and A. M. Stoneham, Philos. Mag. B **60**, 189 (1989)] that thick ($d > 50$ Å) silica films grow by means of interstitial oxygen-molecule diffusion. For thin films (20–50 Å), the experiment using $^{16}O_2$-$^{18}O_2$ isotope oxidation (Ref. [16]) revealed that the mechanism of oxide growth was different from that of thick films. This difference was associated with the transport of oxygen atoms through the oxide network. In both cases, silicon-atom diffusion is found not to limit oxide growth. As to very thin oxide films (< 10 Å), the role of silicon-atom and oxygen-atom transport in silicon oxidation is not clear to date.

[18] V. D. Borman, E. P. Gusev, Yu. N. Devyatko, Yu. Yu. Lebedinskii, S. V. Rogozkin, V. N. Tronin, and V. I. Troyan, Proverkhnost **8**, 22 (1990).

[19] E. P. Gusev and A. P. Popov, Surf. Sci. **248**, 241 (1991).

[20] L. D. Landau and E. M. Lifshitz, *Statistical Physics* (Pergamon, Oxford, 1980), 3rd ed., Vol. 1.

[21] A. Ourmazd, D. W. Taylor, J. A. Rentschler, and J. Bevk, Phys. Rev. Lett. **59**, 213 (1989).

[22] A. Ourmazd, P. H. Fouss, J. Bevk, and J. F. Morar, Appl. Surf. Sci. **41/42**, 365 (1989).

[23] A. V. Emelvanou, Elektron. Promvshlennost **8**, 36 (1983).

[24] A. X. Chu and W. B. Fowler, Phys. Rev. B **41**, 5061 (1990).

[25] Stoneham, Grovenor, and Cerezo (Ref. [17]).

[26] Mott, Rigo, Rochet, and Stoneham (Ref. [17]).